New Data on elastic J/ψ Production from H1 at HERA

Christian Kiesling, for the H1 Collaboration

Max-Planck-Insitute for Physics
Föhringer Ring 6, D-80805 München, Germany

Abstract. New data on cross sections for elastic production of J/ψ mesons in photoproduction and electroproduction are presented for photon virtualities Q^2 up to $80\,\mathrm{GeV}^2$. The photon-proton center-of-mass energy $W_{\gamma p}$ covers the ranges $40 \leq W_{\gamma p} \leq 305\,\mathrm{GeV}$ in photoproduction and $40 \leq W_{\gamma p} \leq 160\,\mathrm{GeV}$ in electroproduction. The steep rise of the cross sections with $W_{\gamma p}$ is confirmed. Differential cross sections $d\sigma/dt$, where t is the squared four-momentum transfer at the proton vertex, are measured in the range $|t| < 1.2\,\mathrm{GeV}^2$ as functions of $W_{\gamma p}$ and Q^2 . An analysis of the J/ψ production and decay angular distributions yields no evidence for a violation of s-channel helicity conservation. The ratio of the cross sections for longitudinal and transverse photons is measured as a function of Q^2 and is found to be described by perturbative QCD models.

Keywords: Total cross sections, differential cross section, meson production
PACS: 13.60Hb, 13.60Le

INTRODUCTION

Quantum Chromodynamics (QCD) is expected to describe the strong force between hadrons, or, at a more fundamental level, between their constituents, the quarks and gluons. QCD is a very successful theory in the limit of short distances, corresponding to small values of the strong coupling constant α_s, where perturbative methods can be applied (perturbative QCD, pQCD). The bulk of the scattering cross section of hadrons, however, is dominated by long-range forces ("soft interactions"), where a satisfactory understanding of QCD still remains a challenge. A large fraction of these soft interactions are mediated by vacuum quantum number exchange and are termed "diffractive". In hadronic interactions, diffraction is well described by Regge theory, which is formulated as a t-channel exchange of a leading trajectory with vacuum quantum numbers, called the "Pomeron" trajectory. In the high energy limit, Pomeron exchange dominates over all other contributions to the scattering amplitude and predicts an almost energy-independent (diffractive) cross section. Elastic scattering is a particular example for such a diffractive process. Measurements of elastic photoproduction $\gamma p \to \mathrm{VM}\ p$ of light vector mesons VM (ρ, ω, and ϕ), which carry the quantum numbers of real photons, $J^{PC} = 1^{--}$, in low Q^2 electron-proton collisions at HERA as function of the photon-proton center-of-mass energy $W_{\gamma p}$ [1, 2] have beautifully verified the expected universal Regge behaviour.

The cross section for elastic photoproduction of J/ψ mesons, $\gamma p \to J/\psi\, p$, on the other hand, was observed [3, 4, 5, 6] to rise steeply with $W_{\gamma p}$, incompatible with a universal Pomeron. Due to its large mass, providing a "hard" scale (equivalent to a short range of the forces involved), the elastic photoproduction of J/ψ mesons is expected to be described by pQCD. This is even more so in electroproduction, where the photon virtuality Q^2 can provide a second hard scale. The presence of two potentially hard scales makes J/ψ production particularly interesting for comparisons with pQCD.

In the past, J/ψ cross sections have been measured (see, e.g., [4, 6, 7, 8, 9, 10, 11]) over a wide range of the photon-proton center-of-mass energy $W_{\gamma p}$ in photoproduction, and in electroproduction spanning the range of photon virtualities up to values of $Q^2 < 100\,\mathrm{GeV}^2$. In this talk more precise data are presented on the Q^2, $W_{\gamma p}$ and t dependence of the cross sections. The data contain up to a factor 3 more integrated luminosity compared to our previous publication [4] for photoproduction and a factor of 2 for electroproduction [7]. The kinematic range has been extended to values of $W_{\gamma p}$ up to 305 GeV in photoproduction, while in electroproduction the range covered now is $40 < W_{\gamma p} < 160\,\mathrm{GeV}$. Furthermore, the angular distributions for production and decay of the J/ψ mesons are determined to extract the cross sections of longitudinal and transverse photons and to test the hypothesis that the helicity of the J/ψ in the final state is the same as that of the initial photon (s-channel helicity conservation, SCHC).

DATA ANALYSIS

The data were recorded by the H1 detector in the years 1999 and 2000 when HERA was operated mostly with positrons. The data sets are selected from an integrated luminosity of 55 pb^{-1}. The J/ψ mesons are detected via their decays into $\mu^+\mu^-$ or e^+e^- pairs in the central and forward tracking detectors (CTD and FTD), as well as in the backward silicon tracker (BST). The scattered positron is detected in the SpaCal calorimeter, while the decay electrons from the J/ψ meson are identified in the LAr and SpaCal calorimeters. Muons are identified as minimum ionizing particles in the LAr calorimeter or in the instrumented iron return yoke (CMD) of the solenoidal magnet which surrounds the central detector. Details on H1 can be found in [12].

In electroproduction the event kinematics is reconstructed using the double angle method. In photoproduction, where the positron is not observed in the central detector, the kinematics is reconstructed from the observed decay particles using the Jaquet-Blondel method [13]. The momentum transfer t is approximated by the transverse momentum of the J/ψ as $t \simeq -\vec{p}_{t,\psi}{}^2$.

Elastic J/ψ production is selected by requiring two leptons (muons or electrons), and a scattered positron in the case of electroproduction. Four data sets are defined covering different regions of Q^2 and $W_{\gamma p}$, corresponding to different signatures of the J/ψ decay leptons and/or the Q^2 range. For the electroproduction and photoproduction at low $W_{\gamma p}$ ($40 < W_{\gamma p} < 160\,\mathrm{GeV}$) the decay channel $J/\psi \to \mu^+\mu^-$ is selected. Exactly two oppositely charged particles must be present in the CTD, with transverse momenta (with respect to the beamline) $p_t > 0.8\,\mathrm{GeV}$. At least one particle must be identified as a muon in the central calorimeter or in the CMD. The details of this analysis can be found in [14]. For the higher $W_{\gamma p}$ energies the electronic decay of the J/ψ is selected. The use of the BST tracks leads to an improved mass reconstruction at the highest values of $W_{\gamma p}$. The details of this analysis can be found in [15].

Monte Carlo simulations are used to calculate the acceptances and efficiencies for triggering, track reconstruction, event selection and lepton identification, both for the signal and for the various QED backgrounds. Systematic uncertainties of the cross sections arise from detector effects which are not perfectly modeled in the simulation of the physics processes. Most uncertainties are obtained by comparisons of data and simulation after tuning the latter with independent data sets.

RESULTS

Cross sections are calculated from the number of selected events after correction for non resonant, proton dissociative and $\psi(2S)$ backgrounds. The MC simulation is used to determine the efficiencies ε for the event selection. Using the integrated luminosity $\mathscr{L}$ and the branching ratio BR for the decay of the J/ψ mesons, the γp cross section is determined in the Weizsäcker-Williams approximation. Cross sections are given at 'bin centers' $\langle W_{\gamma p}\rangle$ and $\langle Q^2\rangle$, which take into account the measured Q^2 and $W_{\gamma p}$ dependences within the bins. The differential cross sections $d\sigma/dt$ are quoted at the weighted mean $\langle t\rangle$ for each t bin, assuming an exponential dependence of the differential cross section with t.

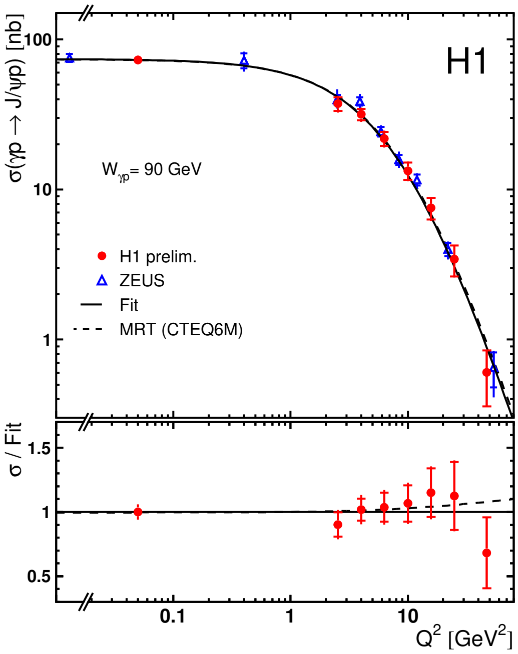

FIGURE 1. Total cross sections for elastic J/ψ production as a function of Q^2 in the range $|t| < 1.2\,\mathrm{GeV}^2$ at $W_{\gamma p} = 90\,\mathrm{GeV}$. The inner error bars show the statistical error, while the outer error bars show the statistical and systematic uncertainties added in quadrature. The solid line is a fit to the H1 data of the form $\sigma_{\gamma p} \propto (M_\psi^2 + Q^2)^{-n}$. Data from the ZEUS experiment [6, 11] are also shown.

A phenomenological fit of the form $\sigma_{\gamma p} \propto (M_\psi^2 + Q^2)^{-n}$ to the H1 data yields a value of $n = 2.486 \pm 0.080(\mathrm{stat.}) \pm 0.068(\mathrm{syst.})$. This result confirms, with smaller errors, the Q^2 dependence observed previously by H1 [7]. The quality of the fit is good (χ^2/ndf= 0.5) and within errors the value of n is independent of the Q^2 range used in the fit. Recent results from the ZEUS collaboration [6, 11] are also shown in figure 1a, which agree well with the present data in the entire range of Q^2.

In figure 1b the pQCD calculations by Martin et al. (MRT [16]) are compared to the fit result quoted above. The predictions are obtained separately for the contributions from transversely and longitudinally polarized photons which are expected to have a different dependence on Q^2. Results using a gluon density distribution (CTEQ6M [17]) derived from global fits to current inclusive F_2 measurements and other data are shown.

$W_{\gamma p}$ **Dependence**: The γp cross section for elastic J/ψ production is presented as a function of $W_{\gamma p}$ in figure 2 for photoproduction. The data are shown with the result of a model independent fit of the form $\sigma_{\gamma p} \propto W_{\gamma p}^{\delta}$ with an empirical parameter δ. The fit yields a value of $\delta = 0.754 \pm 0.033 \pm 0.032$. The first error is obtained using only the statistical uncertainties in the fit. The second quoted error corresponds to the quadratic difference of the two. The total error is obtained by including also the uncorrelated systematic uncertainties added in quadrature. The fit result is in agreement with our previous measurements [4]. Similar data from the ZEUS collaboration [6] (also shown in figure 2) agree well with the present measurements. Two theoretical predictions are compared with the data: The MRT predictions are normalized with the same coefficients as obtained from the comparison of the Q^2 distributions (figure 1). The $W_{\gamma p}$ dependences have also be studied in electroproduction, but are not shown here. Similar conclusions as for photoproduction can be drawn. More comparisons of the MRT model are given in the talk by T. Teubner in these proceedings [18].

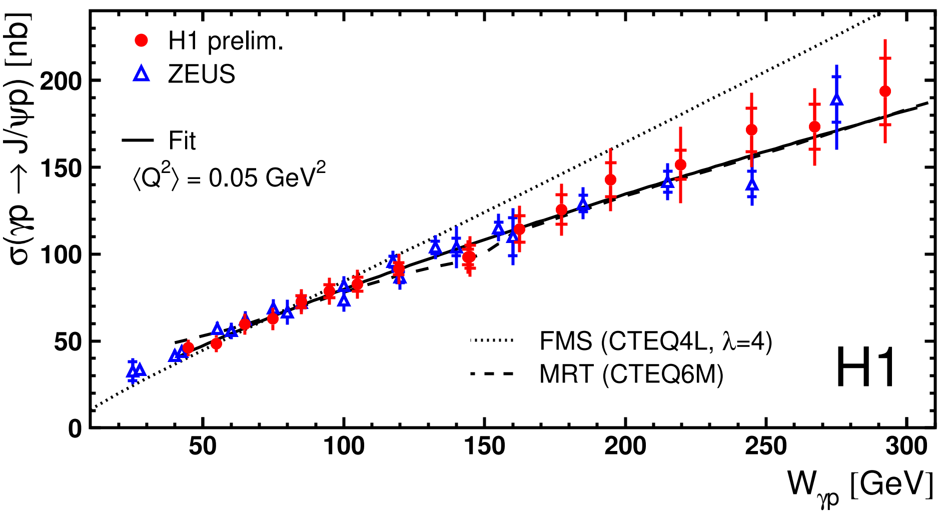

FIGURE 2. Cross sections for elastic J/ψ production as a function of $W_{\gamma p}$ in the range $|t| < 1.2\,\text{GeV}^2$ in photoproduction The solid line shows a fit to the H1 data of the form $\sigma \propto W_{\gamma p}^{\delta}$. Results from the ZEUS experiment [6] in a similar kinematic range are also shown. Predictions from Martin et al. [16] and Frankfurt et al. [19] based on different gluon distributions [17, 20] are shown using the normalization factors determined from the Q^2 distributions.

Differential Cross Sections: The t dependence of the elastic cross section for J/ψ meson production has been studied for photoproduction and for electroproduction in the range $40 < W_{\gamma p} < 160\,\text{GeV}$ for different Q^2 bins. For photoproduction, the measurement of the t dependence has been extended to significantly higher $W_{\gamma p}$ (up to $W_{\gamma p} = 305$

GeV). The differential cross sections $d\sigma/dt$ are well described by single exponentials ($\chi^2/\mathrm{ndf} = 0.25$, e.g. in the case of photoproduction). In the context of developing the calculations using generalized parton densities, Frankfurt and Strikman [21] have proposed an alternative shape. It is based on a dipole function with a t dependent two-gluon form factor $d\sigma/dt \propto (1 - t/m_{2\mathrm{g}}^2)^{-4}$. In a fit to the photoproduction data the two-gluon invariant mass $m_{2\mathrm{g}}$ is left as a free parameter. This form is strongly disfavored by the data ($\chi^2/\mathrm{ndf} = 5.48$).

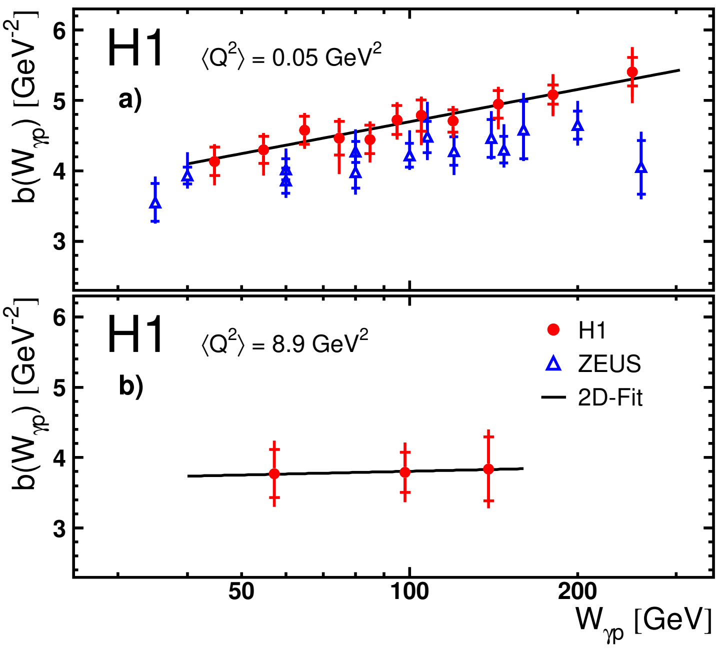

FIGURE 3. The values of the t slope $b(W_{\gamma p})$ as a function of $W_{\gamma p}$in the range $|t| < 1.2\,\mathrm{GeV}^2$ for a) photoproduction and b) electroproduction. $\langle Q^2 \rangle$ indicates the bin center value in the Q^2 range considered. The data points are the results of one-dimensional fits of the form $d\sigma/dt \propto e^{bt}$ in $W_{\gamma p}$ bins. The solid lines show the results of the two-dimensional fits. In figure a) the data are compared to results by the ZEUS collaboration [6].

Exponential fits of the form e^{bt} to the measured differential cross sections $d\sigma/dt$ in bins of $W_{\gamma p}$ are performed and the resulting values for b are displayed in figure 3a and b for photo- and electroproduction, respectively. For photoproduction the b values are seen to increase with $W_{\gamma p}$. These b slope values are independent of normalization uncertainties between data sets. The curves in figure 3a and b show the corresponding result $b(W_{\gamma p})$ from a two-dimensional fit in $W_{\gamma p}$ and t. They agree well with the data.

In figure 3a photoproduction results for the slope parameter from the ZEUS experiment [6] in a similar kinematic region are also shown. They show a similar dependence on $W_{\gamma p}$ but are on average 0.5 GeV^{-2} lower. This difference in the absolute size of b may be due to differences in the handling of the background from proton dissociative events, which has a much shallower b slope ($1.6\,\mathrm{GeV}^{-2}$[9]).

Studies of the production and decay angles of the J/ψ yield consistency with s-channel helicity conservation (SCHC) within experimental errors (the corresponding new data are not shown). In the case of SCHC a direct measurement of R, the ratio of

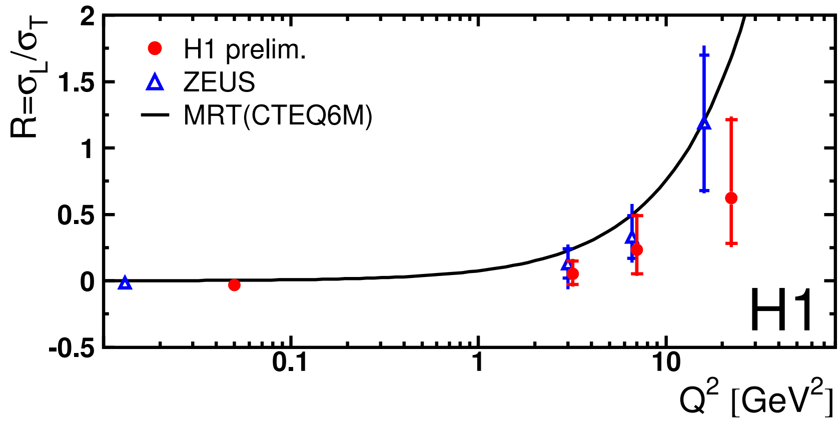

FIGURE 4. Ratio $R = \sigma^L/\sigma^T$ as a function of Q^2 (deduced from the measurement of r^{04}_{00} from the $\cos\theta^*$ distribution) for the range $40 < W_{\gamma p} < 160\,\mathrm{GeV}$ and $|t| < 5\,\mathrm{GeV}^2$. The data are compared to the result of a calculation by Martin et al. [16] based on the CTEQ6M [17] gluon distribution. Also shown are results from the ZEUS collaboration [6, 11].

the cross sections for longitudinal and transverse photons, σ^L and σ^T respectively, can be performed (see figure 4). For comparison the prediction from MRT [16] is shown, which depends only weakly on the particular gluon density. Here, the gluon density from CTEQ6M is chosen, which gives the best description of the Q^2 and $W_{\gamma p}$ dependences of the cross sections. The data are described reasonably well. Similar measurements from [6, 11] agree well with the present data.

SUMMARY

New measurements of elastic J/ψ photoproduction and electroproduction in the range $40 < W_{\gamma p} < 305\,\mathrm{GeV}$ have been presented. The cross section $\sigma(\gamma p \to J/\psi p)$ is measured as a function of Q^2 in the range $0 < Q^2 < 80\,\mathrm{GeV}^2$, and a fit of the form $\sigma_{\gamma p} \propto (M_\psi^2 + Q^2)^{-n}$ yields $n = 2.486 \pm 0.080(\mathrm{stat.}) \pm 0.068(\mathrm{syst.})$. The shape of the Q^2 distribution is well described by a perturbative QCD calculation by Martin et al. [16], almost independent of the gluon density distribution used.

The photoproduction cross section is measured as a function of the photon-proton center-of-mass energy $W_{\gamma p}$ in the range $40 < W_{\gamma p} < 305\,\mathrm{GeV}$, and is parameterized as $\sigma_{\gamma p} \propto W_{\gamma p}^{\delta}$ with $\delta = 0.754 \pm 0.033 \pm 0.032$. The results for δ in electroproduction, measured in the range $40 < W_{\gamma p} < 160\,\mathrm{GeV}$, are consistent with those in photoproduction and no change with Q^2 is observed within experimental errors.

Predictions of the $W_{\gamma p}$ dependence of the cross section in pQCD-based models seem to depend strongly on the form of the gluon distribution, as was observed explicitely in the model of Martin, Ryskin and Teubner: A good description of the shape of the data can currently be achieved only with some gluon distributions. This may demonstrate the high potential of constraining the gluon distribution with the elastic J/ψ data in a kinematic region (low x, low Q^2) where fits from inclusive data yield gluon distributions with very large uncertainties.

The differential cross section $d\sigma/dt$ for elastic J/ψ photoproduction for $|t| \leq 1.2\,\mathrm{GeV}^2$ has been extended to the full $W_{\gamma p}$ range of HERA, $40-305\,\mathrm{GeV}$, in photoproduction. The differential cross sections $d\sigma/dt$ are well parameterized as a single exponential, dipole forms are strongly disfavored. The slope parameter shows a dependence on $W_{\gamma p}$, which is weaker than expected from soft Pomeron phenomenology, but is clearly positive, leading to a shrinkage of the forward scattering peak. The slope parameters in electroproduction agree with photoproduction within errors, but have a tendency to decrease with Q^2 .

Finally, the helicity structure of diffractive J/ψ production is analyzed as a function of Q^2 and $|t|$. No evidence is found for a violation of s-channel helicity conservation (SCHC). Assuming SCHC, the ratio of the longitudinal to the transverse cross section is determined as a function of Q^2 and is found to be reasonably well described by QCD calculations.

ACKNOWLEDGMENTS

We very much appreciated the pleasant and stimulating atmosphere of this workshop, as well as the splendid organisation by the local committee from Madison University. We also thank T. Teubner and M. Strikman for valuable discussions and for making their theoretical predictions available.

REFERENCES

1. S. Aid *et al.*, H1 Collaboration, *Nucl. Phys. B*, **468**, 3 (1996).
2. M. Derrick *et al.*, ZEUS Collaboration, *Z. Phys. C*, **69**, 39 (1995).
3. S. Aid *et al.*, H1 Collaboration, *Nucl. Phys. B*, **472**, 3 (1996).
4. C. Adloff *et al.*, H1 Collaboration, *Phys. Lett. B*, **483**, 23 (2000).
5. J. Breitweg *et al.*, ZEUS Collaboration, *Z. Phys. C*, **75**, 215 (1997).
6. S. Chekanov *et al.*, ZEUS Collaboration, *Eur. Phys. J. C*, **24**, 345 (2002).
7. C. Adloff *et al.*, H1 Collaboration, *Eur. Phys. J. C*, **10**, 373 (1999).
8. C. Adloff *et al.*, H1 Collaboration, *Phys. Lett. B*, **541**, 251 (2002).
9. A. Aktas *et al.*, H1 Collaboration, *Phys. Lett. B*, **568**, 205 (2003).
10. J. Breitweg *et al.*, ZEUS Collaboration, *Eur. Phys. J. C*, **6**, 603 (1999).
11. S. Chekanov *et al.*, ZEUS Collaboration, *Nucl. Phys. B*, **695**, 3 (2004).
12. I. Abt *et al.*, H1 Collaboration, *Nucl. Instrum. Meth. A*, **386**, 310 (1996).
13. F. Jacquet, and A. Blondel, "The Kinematics of *ep* Interactions," in *Study for an ep Facility for Europe*, edited by U. Amaldi, DESY-79-048, 1979.
14. P. Fleischmann, *Elastic J/ψ Production at HERA*, Ph.D. thesis, Universität Hamburg, Hamburg (2004).
15. L. Janauschek, *Elastic Photoproduction of J/ψ Vector Mesons at High Photon-Proton Center of Mass Energies at the H1 Experiment at HERA*, Ph.D. thesis, Ludwig-Maximilians-Universität, München (2004).
16. A. D. Martin, M. G. Ryskin, and T. Teubner, *Phys. Rev. D*, **62**, 014022 (1999).
17. J. Pumplin *et al.*, *JHEP*, **0207**, 012 (2002).
18. T. Teubner, *these proceedings* (2005).
19. L. Frankfurt, M. McDermott, and M. Strikman, *JHEP*, **0103**, 045 (2001).
20. A. D. Martin, R. G. Roberts, W. J. Stirling, and R. S. Thorne, *Eur. Phys. J. C*, **23**, 73 (2002).
21. L. Frankfurt, and M. Strikman, *Phys. Rev. D*, **66**, 031502 (2002).